

Influence of Capacitive Effects on Transformer Windings

Mathurin Gogom*, Rodolphe Gomba, Desire Lilonga-Boyenga

Polytechnical Superior National School, Marien Ngouabi University, Brazzaville, Congo

Email: *mathuringogom@gmail.com

How to cite this paper: Gogom, M., Gomba, R. and Lilonga-Boyenga, D. (2021) Influence of Capacitive Effects on Transformer Windings. *Energy and Power Engineering*, 13, 67-80.

<https://doi.org/10.4236/epe.2021.132005>

Received: June 4, 2020

Accepted: January 31, 2021

Published: February 3, 2021

Copyright © 2021 by author(s) and Scientific Research Publishing Inc.

This work is licensed under the Creative Commons Attribution International License (CC BY 4.0).

<http://creativecommons.org/licenses/by/4.0/>



Open Access

Abstract

For years, capacitive effects have been the subject of research [1] and [2]. The capacitive effects are discrete capacitors that appear between active conductors of power lines and between them with the ground plane, generating capacitive reactive power to the network [1] and [2]. Indeed, it must be noted that these effects affect the windings of the transformer when the coupling is in star or triangle. This study is conducted to show that capacitive effects affect transformer windings differently when coupling is in stars or triangles. The results obtained are interesting and can be exploited in electrical transmission networks to ensure a long lifespan of transformers.

Keywords

Capacitive Effects, Discrete Capacitors, Geometry of Conductors, Transformers Windings

1. Introduction

The transport of electrical energy between production and consumption centres, often characterized by long distances, poses many problems, among other things, joule losses and voltage drops [3] [4] [5] [7] and [8]. To this end, several works have been carried out, including the optimization of joule losses and voltage drops through traditional or advanced compensation of reactive power [3] [4] [5] [6] and [7]. However, work on the impact of capacitive effects is still very limited, requiring special attention.

Indeed, the reactive energy generated by discrete capacitors that are created between the different active conductors on the one hand, and between each active conductor with the plane of the ground on the other hand, varies according to the configuration (geometry) of the line. This generated reactive energy is distributed in half on each of the two ends of the line or cable [8] and [10].

When not consumed, this reactive energy generated becomes one of the causes of unwanted surges and therefore instability of the voltage of the network. These capacitive effects are very harmful when operating empty or low-load transportation system [11] [12] and [13]. These capacitive effects have a different impact on the transformer windings connected to the power transmission lines. This difference is due to the way the coils are paired.

The formation of these discrete capacitors reflects the capacitive effects on electrical lines and cables. The reactive power absorbed by the inductions of the lines or debited by the capacitors thus formed must obey the requirements of the networks, including the stability and reliability of the transport networks.

The interest of this work is to show how discrete capacitors affect transformers' coils differently because of their coupling. Therefore, special attention must be paid to the selection of the cutting of the windings of transformers operated in the transmission networks of electrical energy.

2. Theoretical Study

2.1. Capacitors Illustrations

A high voltage power line generates reactive energy because of the capacitors that form between the different conductors on the one hand, and between each conductor and the ground plane on the other hand, as illustrated in **Figure 1** [3] and [4].

Indeed, the capacitor which forms between two conductors (1) and (2) for example, generates reactive power Q_{12} to the network. Between the different line conductors, we have capacitors C_{12} , C_{23} and C_{13} , and between each line conductor and the ground plane the capacitors C_{10} , C_{20} and C_{30} .

2.2. Reactive Power Generated

The example of the plug circuit makes us understand that the capacitor sends its energy on the impedance which is in parallel with it; this allows us to deduce that among the various capacitors formed between the lines conductors, some generate undesirable reactive energy on the transformers windings at the level of the departure and arrival stations when the line is operating at empty or at low load.

The power generated by the capacitor formed between the two conductors (i) and (j) as shown in **Figure 2**, is found in half on each end of the section, that means $Q_{ij}/2$ on each end [3] and [4].

2.2.1. Triangle Transformer Coupling

1) Reactive powers generated

It is established that the various capacitors formed between the line conductors appear as reactive energy sources as illustrated in **Figure 3**. They respectively supply impedances in parallel, in particular the transformer windings.

For a capacitor created between the active line conductor and the ground

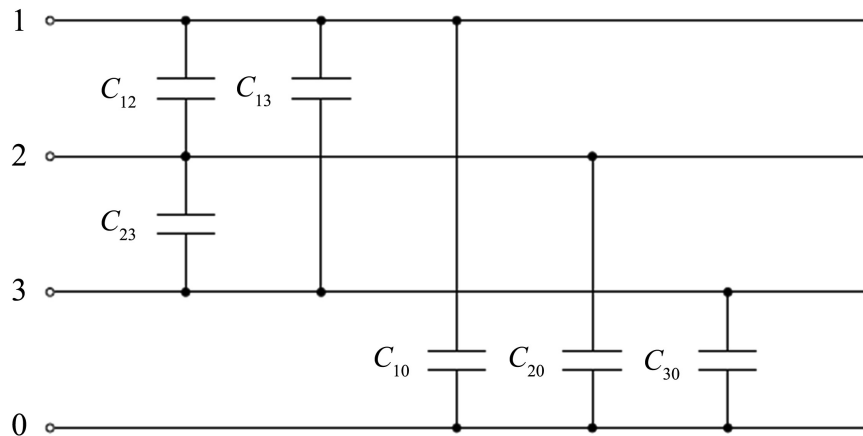


Figure 1. Capacities formed on a power line.

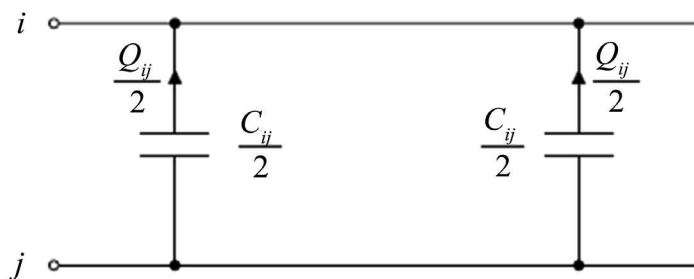


Figure 2. Distribution of reactive energy at the ends of the line.

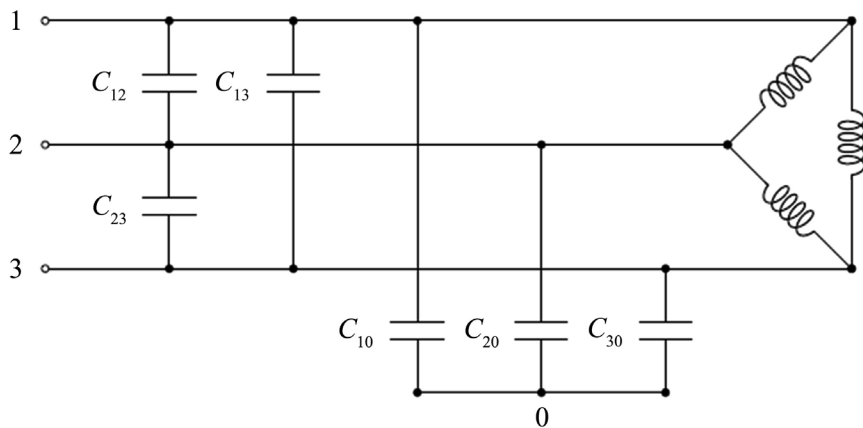


Figure 3. Case of coupling transformer's windings in triangle.

plane, the reactive power generated by these different capacitors is located between the phases and the ground plane. This reactive power is that which can be consumed by the equipment which are in parallel with them located at the entrance to the transformer station if these exist. The expression of this reactive power is given by the relation (1) below [1] [2]:

$$Q_{i0} = 3C_{i0}\omega V_{i0}^2 \tag{1}$$

where V_{i0} is the simple voltage of module $V_{i0} = \frac{U_{12}}{\sqrt{3}} = \frac{U_{13}}{\sqrt{3}} = \frac{U_{23}}{\sqrt{3}}$ et $i = 1, 2$

and 3;

For the capacitors formed between the guard cables and the ground plane, it can be said that all the energy is earthed, because the two plates constituting this capacitor are earthed; regarding the capacitor created between an active conductor and the guard wire, we find ourselves in the case of a capacitor armature which is connected to earth. Here, we join the previous case where the power generated by the capacitor is sent to earth.

In the case of the capacitor formed between two guard cables, the two armatures of the capacitor thus formed are connected to the ground through pylons. The reactive energy generated is well flowed to the earth;

Regarding the capacitors formed between active conductors, the reactive powers generated by the three capacitors created between the two active conductors of the line are such that:

$$Q_{12} = C_{12}\omega(U_{12})^2, \quad Q_{13} = C_{13}\omega(U_{13})^2 \quad \text{et} \quad Q_{23} = C_{23}\omega(U_{23})^2 \quad (2)$$

At the start station, this reactive power generated by the capacitors of the line is consumed by the secondary winding of the transformer while at the arrival station; this reactive power is consumed by the primary winding of the transformer at this station. Then we can write [1] [2]:

$$Q_{12} = \frac{U_{12}^2}{L_{12}\omega} \quad \text{then} \quad L_{12} = \frac{U_{12}^2}{Q_{12}\omega^2} \quad (3)$$

$$Q_{13} = \frac{U_{13}^2}{L_{13}\omega} \quad \text{then} \quad L_{13} = \frac{U_{13}^2}{Q_{13}\omega^2} \quad (4)$$

$$Q_{23} = \frac{U_{23}^2}{L_{23}\omega} \quad \text{then} \quad L_{23} = \frac{U_{23}^2}{Q_{23}\omega^2} \quad (5)$$

2) Equivalent capacities

For the purposes of modeling a power line in T or in π , the value of the capacity C to be taken into account per phase is the capacity resulting from the transformation of **Figure 4**.

The triangle formed by nodes 1, 2 and 3 can be reduced to the star shape by the triangle-star transformation. The point "n" is at the same potential as the earth, the values of C_{1n} , C_{2n} and C_{3n} are given by [8]: (**Figure 5**)

$$C_{1n} = C_{12} + C_{13} + \frac{C_{12}C_{13}}{C_{23}} \quad (6)$$

$$C_{2n} = C_{12} + C_{23} + \frac{C_{12}C_{23}}{C_{13}} \quad (7)$$

$$C_{3n} = C_{13} + C_{23} + \frac{C_{13}C_{23}}{C_{12}} \quad (8)$$

We arrive at the final equivalent diagram of **Figure 6** of which $C_{\acute{e}q1}$, $C_{\acute{e}q2}$ and $C_{\acute{e}q3}$ are given by the expressions below:

$$C_{\acute{e}q1} = C_{1n} + C_{10} \quad (9)$$

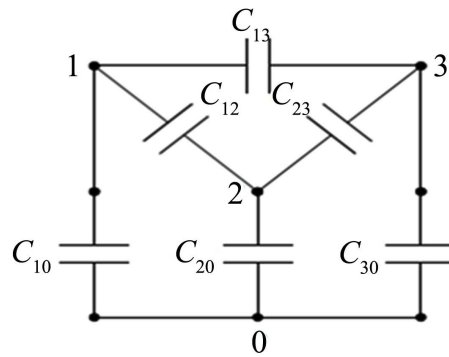


Figure 4. Simplified diagram of a dull simple line.

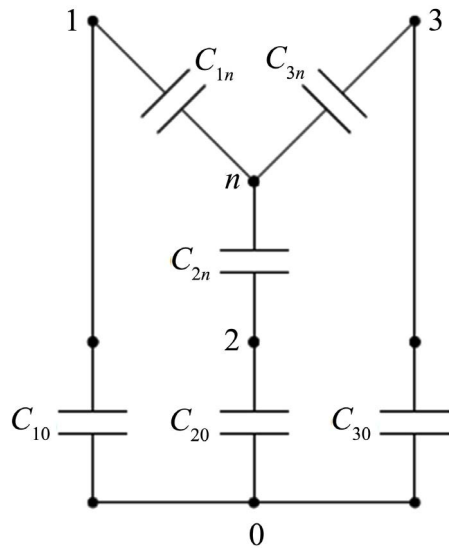


Figure 5. Equivalent diagram in star.

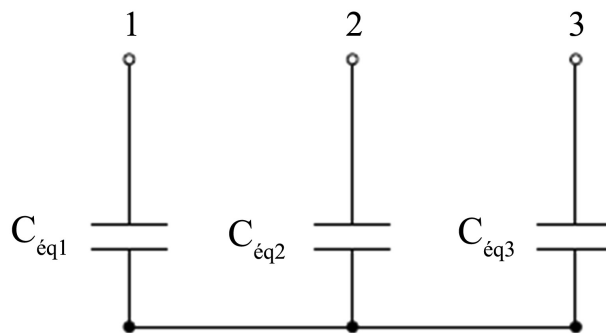


Figure 6. Final equivalent diagram.

$$C'_{eq2} = C_{2n} + C_{20} \tag{10}$$

$$C'_{eq3} = C_{3n} + C_{30} \tag{11}$$

2.2.2. Star Transformer Coupling

1) Reactive power generated

As in the previous case, the different capacitors formed act in the same way.

They feed the impedances which are parallel to them (Figure 7).

For a capacitor created between the line active conductor and the ground, the reactive power generated by these different capacitors is located between the phases and the ground. This reactive power is that consumed by half the transformers windings of the upstream and downstream stations of the line. It is given by the relation:

$$Q_{i0} = 3C_{i0}\omega V_{i0}^2 \tag{12}$$

where V_{i0} is the simple voltage for which the module is given by

$$V_{i0} = \frac{U_{12}}{\sqrt{3}} = \frac{U_{13}}{\sqrt{3}} = \frac{U_{23}}{\sqrt{3}}, \quad i = 1, 2 \text{ and } 3;$$

As for the capacitors formed between the guard cables and the ground, all of the reactive energy is earthed; Regarding the capacitor created between an active conductor and the guard wire, all reactive energy is discharged to the earth; In the case of the capacitor formed between two guard cables, the reactive energy generated is well drained to the earth; As regards the capacitors formed between two active conductors, the reactive powers generated by each capacitor are such that:

$$Q_{12} = C_{12}\omega(U_{12})^2, \quad Q_{13} = C_{13}\omega(U_{13})^2, \quad Q_{23} = C_{23}\omega(U_{23})^2 \tag{13}$$

At the start station, half of this reactive power generated by the capacitors formed between line active conductors is consumed by the two secondary windings of the transformer; and at the arrival station, the other half of this reactive power is consumed by the two primary windings of the transformer at this station. Each winding consumes:

$$Q_1 = L_1\omega I_1^2 = \frac{V_1^2}{L_1\omega} \tag{14}$$

$$Q_2 = L_2\omega I_2^2 = \frac{V_2^2}{L_2\omega} \tag{15}$$

$$Q_{12} = Q_1 + Q_2 \tag{16}$$

We deduce successively:

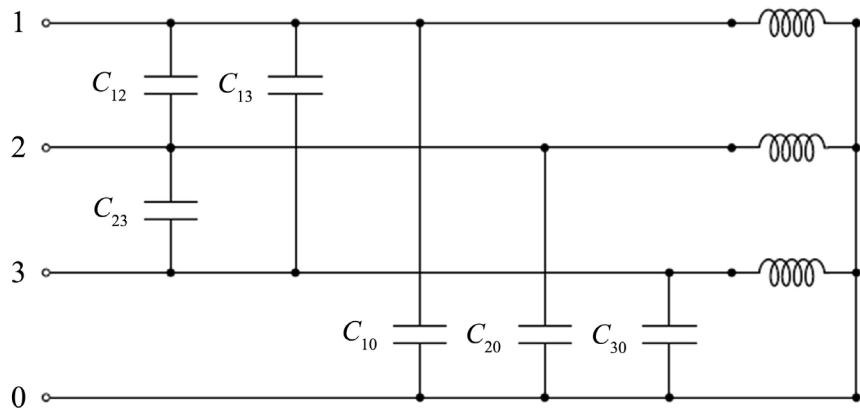


Figure 7. Line supplying the windings of a star-mounted transformer.

$$Q_{12} = \frac{V_1^2}{L_1\omega} + \frac{V_2^2}{L_2\omega} \quad (17)$$

$$Q_{13} = \frac{V_1^2}{L_1\omega} + \frac{V_3^2}{L_3\omega} \quad (18)$$

$$Q_{23} = \frac{V_2^2}{L_2\omega} + \frac{V_3^2}{L_3\omega} \quad (19)$$

2) Equivalent capacities

For modeling purposes of a power line in T or π , the value of the capacitance C to be taken into account per phase is the capacitance resulting from the transformation of **Figure 8** below.

For modeling purposes of a power line in T or π , the value of the capacitance C to be taken into account per phase is the capacitance resulting from the transformation of **Figure 8** below.

The triangle formed by nodes 1, 2 and 3 can be reduced to a star shape by the triangle-star transformation. The point "n" is at the same potential as the earth, the values of C_{1n} , C_{2n} and C_{3n} are given by: (**Figure 9**)

$$C_{1n} = C_{12} + C_{13} + \frac{C_{12}C_{13}}{C_{23}} \quad (6')$$

$$C_{2n} = C_{12} + C_{23} + \frac{C_{12}C_{23}}{C_{13}} \quad (7')$$

$$C_{3n} = C_{13} + C_{23} + \frac{C_{13}C_{23}}{C_{12}} \quad (8')$$

We arrive at the following final equivalent diagram: (**Figure 10**)

Under the balanced three-phase regime hypothesis, point n is at the same potential as earth, thus:

$$C_{\acute{e}q1} = C_{1n} + C_{10} \quad (9')$$

$$C_{\acute{e}q2} = C_{2n} + C_{20} \quad (10')$$

$$C_{\acute{e}q3} = C_{3n} + C_{30} \quad (11')$$

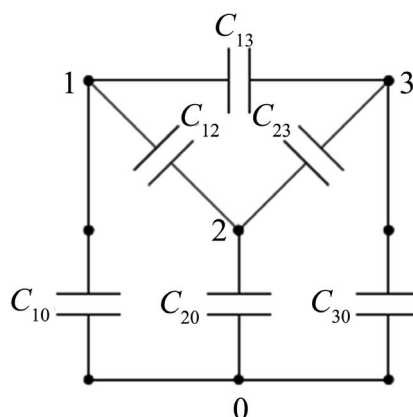


Figure 8. Simplified diagram of a dull single line.

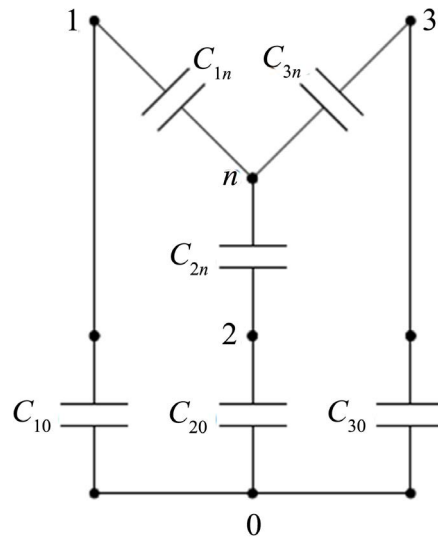


Figure 9. Equivalent diagram in star.

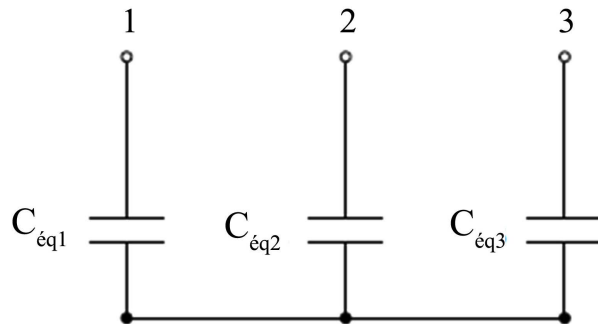


Figure 10. Final equivalent diagram.

2.3. Capacitor Capacity

It is a question of giving the expressions of the capacitors capacities formed between the line active conductors on the one hand, and between line active conductor with the ground plane on the other hand by taking into account the geometry of the lines. The capacity of a capacitor formed between two active conductors is given by [11] [12] [13]:

$$C_{ij} = \frac{\pi \epsilon_0}{\log \left[\frac{D_{ij} + \sqrt{\frac{D_{ij}^2}{4} + r^2}}{r} \right]} \quad (20)$$

However, that of a capacitor formed between the active conductor and the ground plane is given by [11] [12] [13]:

$$C_{i0} = \frac{2\pi \epsilon_0}{\log \left[\frac{h_{i0} + \sqrt{h_{i0}^2 + r^2}}{r} \right]} \quad (21)$$

where:

D_{ij} , the distance between two active conductors; r , conductor radius; ε_0 , absolute permittivity in a vacuum ($\varepsilon_0 = 8.854 \times 10^{-12}$ F/m) and h_0 , the distance between the active conductor and the ground plane.

3. Determination of Reactive Capacities and Powers

3.1. Reactive Capacities and Powers

We use formulas (2), (12), (13), (20) and (21) to calculate the capacities and the reactive powers generated C_{ij} , C_0 , Q_{ij} and Q_0 as a function of the voltage level and the geometry of the single term line conductors; the distance between two active conductors, the radius of the conductor and the distance between the active conductor on the ground plane. The results obtained are reported in **Table 1** and **Table 2** below.

We note, from the results recorded in **Table 1**, that the capacities C_{ij} and C_0 are not the same; they vary according to the geometry of the line conductors. The reactive powers Q_{ij} and Q_0 generated vary in the same way. It should also be noted that the reactive power generated by the capacitor formed between the active conductor and the ground plane decreases as the height between them increases. Similarly, that generated by the capacitors formed between active conductors decreases when the distance between them increases.

3.2. Equivalent Capacities and Reactive powers

The formulas (6), (7), (8), (9), (10), (11) and (12) enabled us to calculate the equivalent capacities values of the capacitors thus formed for each voltage level. However, formulas (1) and (12) allowed us to calculate the reactive powers generated per phase. The results obtained are presented in **Table 3**.

For each given voltage level, the equivalent capacities C_{eqi} and the reactive powers generated Q_i differ from one geometry of the line conductors to another. Likewise, the equivalent capacities and the reactive powers generated differ from one phase to another. With regard to the results in **Table 4**, we note that the windings of the transformers consume different reactive powers.

Table 1. Capacitance values of capacitors formed.

Capacitance	110 KV			220 KV		
	Nappe	Equilateral Triangle	Isocel Triangle	Nappe	Equilateral Triangle	Isocel Triangle
C_{12} (10^{-12} F/m)	10.144	10.144	10.144	9.6136	9.6136	9.6136
C_{13} (10^{-12} F/m)	9.1405	10.144	9.616	8.7076	9.6136	9.1382
C_{23} (10^{-12} F/m)	10.144	10.144	10.144	9.6136	9.6136	9.6136
C_{10} (10^{-12} F/m)	15.198	15.198	14.876	15.251	15.251	14.799
C_{20} (10^{-12} F/m)	15.198	14.647	15.198	15.251	14.501	15.251
C_{30} (10^{-12} F/m)	15.198	15.198	15.198	15.251	15.251	15.251

Table 2. Reactive powers values generated.

Reactive powers	110 KV			220 KV		
	Nappe	Equilateral Triangle	Isocel Triangle	Nappe	Equilateral Triangle	Isocel Triangle
Q_{12} (KVAR/Km)	38.541	38.541	38.541	146.104	146.104	146.104
Q_{13} (KVAR/Km)	34.728	38.541	36.535	132.336	146.104	138.879
Q_{23} (KVAR/Km)	38.541	38.541	38.541	146.104	146.104	146.104
Q_{10} (KVAR/Km)	57.745	57.745	56.522	231.777	231.777	224.923
Q_{20} (KVAR/Km)	57.745	55.651	57.745	231.777	220.376	231.777
Q_{30} (KVAR/Km)	57.745	57.745	57.745	231.777	231.777	231.777

Table 3. Equivalent capacitance values of the capacitors formed.

Equivalent capacitance	110 KV			220 KV		
	Nappe	Equilateral Triangle	Isocel Triangle	Nappe	Equilateral Triangle	Isocel Triangle
$C_{eq,1}$ (10^{-12} F/m)	43.6235	45.63039	44.2529	42.2799	44.0918	41.8289
$C_{eq,2}$ (10^{-12} F/m)	45.6304	45.07924	46.1872	45.0920	43.3416	44.5919
$C_{eq,3}$ (10^{-12} F/m)	43.6235	45.63039	44.5747	42.2799	44.0918	43.1410

Table 4. Reactive power values generated per phase.

Reactive power	110 KV			220 KV		
	Nappe	Equilateral Triangle	Isocel Triangle	Nappe	Equilateral Triangle	Isocel Triangle
Q_1 (KVAR/Km)	165.7431	173.3681	168.1345	672.1592	670.0896	635.6988
Q_2 (KVAR/Km)	173.3681	171.2741	175.4836	685.2900	658.6884	677.6898
Q_3 (KVAR/Km)	165.7431	173.3681	169.3571	642.5528	670.0896	655.6396

3.3. Application to the Radial Network

The influence of capacitive effects on the windings of the transformers located upstream and downstream of the lines is examined on the Liouesso-Ouessou network in the Sangha department of the Republic of Congo.

3.3.1. Network Description

The Liouesso-Ouessou electrical network is shown in **Figure 11**. These characteristics are summarized in **Table 5**.

3.3.2. Network Modeling

We possibly choose the basic voltage and power to transcribe the network parameters in pu [9]. So, $U_B = 110$ KV; $S_B = 100$ MVA and we deduce the basic impedance and admittance such as: $Z_B = \frac{U_B^2}{S_B}$ et $Y_B = \frac{S_B}{U_B^2}$. These parameters are presented in **Table 6** and **Table 7** below:

Table 5. (a) Characteristics of the Liouesso-Ouesso network; (b) Continuation of the characteristics of the Liouesso-Ouesso network.

(a)								
Alternators				Transformation post of Liouesso				
U_n	$3 \times S_n$	$\cos\varphi$	$3 \times P_n$	U_{1n}	U_{2n}	S_n	U_{ncc}	P_{ncc}
kV	MVA	-	MW	KV	KV	MVA	%	KW
11	23.43	0.85	19.5	11	110	25	10.5	29

(b)								
Ligne 110 kV				Transformation post of Ouesso				
L	r_0	x_0	b_0	U_{1n}	U_{2n}	S_n	U_{ncc}	P_{ncc}
Km	Ω/Km	Ω/Km	Ω^{-1}/Km	KV	KV	MVA	%	KW
120	0.17	0.39	$2.95 \cdot 10^{-6}$	110	20	25	10.5	60

Table 6. Longitudinal and transverse parameters of the line in pu.

No.	Sections	R	X	G	B
1	1 - 2	0.025	0.27	0	0
2	2 - 3	0.17	0.4	0	0.43
3	3 - 4	0.012	0.09	0	0

Table 7. Active and reactive powers at the nodes of the pu network.

No.	P_G	Q_G	P_C	Q_C
1	0	0		
2			0	0
3			0	0
4			0	0

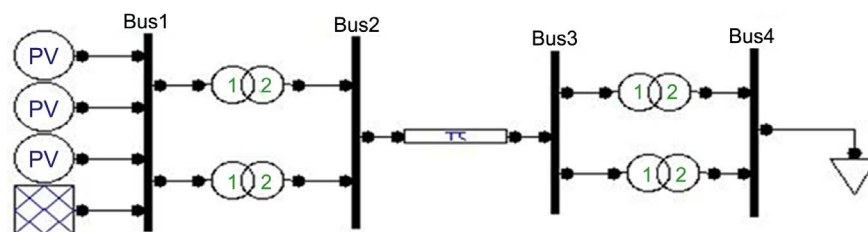


Figure 11. “Liouesso-Ouesso” Electrical network.

3.3.3. Simulations, Results and Discussion

The simulations are performed during no-load operation using the Newton-Raphson algorithm implemented in Matlab [9]. The results obtained are presented in the following **Table 8**.

From the results obtained, we can deduce the reactive powers generated by the capacitors formed between conductors using formula (2). These are presented in **Table 9** below. At the end of these deductions, we will appreciate the influence

of these capacitive effects on the transformers windings located upstream and downstream of the line.

3.3.4. Inductance Deduction

It is interesting to appreciate the inductances of the transformers windings which consume the reactive energy generated by the capacitors thus formed. The consumption of this energy varies according to the coupling of the windings.

1) Triangle coupling of windings

By applying formulas (3), (4) and (5), we obtain the results given in **Table 10** below:

2) Star coupling of windings

Assuming that the system is symmetrical, solving Equations (17), (18) and (19) allows us to obtain the results recorded in **Table 11** below:

The examination of the results recorded in **Table 10** and **Table 11** show that the geometry of the conductors in an equilateral triangle guarantees the symmetry of the three-phase system; however, the star coupling is more expensive, because the windings of this one can have a number of turns $\sqrt{3}$ times less than that of the transformer whose coupling of the windings is in triangle.

Table 8. Voltage modules and phases, then powers generated and consumed at the nodes in pu.

No.	V	φ	P_G	Q_G	P_C	Q_C
1	1.0200	0	0.0195	-0.5323		
2	1.1606	-0.0157			0	0
3	1.2688	-0.0556			0	0
4	1.2688	-0.0556			0	0

Table 9. Reactive powers generated during no-load operation.

Reactive powers	110 KV		
	Nappe	Equilateral Triangle	Isocel Triangle
Q_{12} (MVAR)	7.4454	7.4454	7.4454
Q_{13} (MVAR)	6.7089	7.4454	7.0579
Q_{23} (MVAR)	7.4454	7.4454	7.4454

Table 10. Inductances values of the windings transformer.

Inductances	110 KV		
	Nappe	Equilateral Triangle	Isocel Triangle
L_{12} (H)	8.3321	8.3321	8.3321
L_{23} (H)	8.3321	8.3321	8.3321
L_{13} (H)	9.2468	8.3321	8.7895

Table 11. Inductances values of the transformer's windings.

inductances	110 KV		
	Nappe	Equilateral Triangle	Isocel Triangle
L_1 (H)	2.777	2.777	2.777
L_2 (H)	3.082	2.777	2.929
L_3 (H)	2.777	2.777	2.777

4. Conclusions

In our study, we first modeled the line by essentially representing discrete capacitors between active conductors on the one hand, and between active conductors and the ground on the other. Then we calculated the capabilities of discrete capacitors. Similarly, equivalent capacities were deducted. In the end, the examination of the influence of capacitive effects on transformer coils was done on the existing radial power grid in the Republic of Congo. The results show that:

- Discrete capacitors generate reactive energies that vary depending on the geometry of line conductors;
- Capacitive effects affect transformer coils differently depending on whether the coupling is in a triangle or a star;
 - For triangle coupling, the coiling of the transformer's coil consumes all of the energy generated;
 - For star coupling, the energy generated is consumed by the two coils of the transformer's coils.

In short, the design of line conductors in equilateral triangle is ideal compared to other models when it comes to ensuring the symmetry of the three-phase system. However, star coupling is more advantageous than triangle coupling, as the number of coils spins is reduced by $\sqrt{3}$ times and the coil induction will be 3 times smaller, and therefore the star coupling guarantees a long life of the transformer compared to the one whose coupling is in a triangle.

Conflicts of Interest

The authors declare no conflicts of interest regarding the publication of this paper.

References

- [1] Lyazid, H. and Khodir, H. (2015) Calcul des Paramètres et Caractéristiques des Lignes Électriques Triphasées. Mémoire de Master 2 Génie Électrique, Université Abderrahmane Mira, Béjaïa.
- [2] Wildi, T. and Sibille, G. (2005) Electrotechnique. 4^e Édition, Presses de l'Université Laval, Québec.
- [3] Abba Labane, H. and Omboua, A. (2016) Capacitive Dividers on the High Voltage Lines. *International Journal of Engineering and Advanced Research Technology*, **2**, 26-32.
- [4] Abba Labane, H., Omboua, A. and Lilonga-Boyenga, D. (2017) Capacitive Effects

- on Electrical Lines and Cables. *International Journal of Engineering Science Invention*, **6**, 25-32.
- [5] Sayah, A. (2017) Analyse des Terminaisons d'Eau. Thèse de l'Université des Sciences et de la Technologie d'Oran Mohamed Boudiaf, Bir El Djir.
- [6] Omboua, A. (2017) Soutirage de l'Énergie le Long des Lignes à Haute Tension: Technologie Profitable Pour les Pays en Développement. *International Journal of Innovation and Applied Studies*, **20**, 349-357.
- [7] Lagonotte, P. (2004) Les Lignes et Des Câbles Électriques. In *Chapitre 10 du Cours de Réseaux Électrique*.
- [8] Yalaoui, N. (2017) Calcul de la Matrice d'Impédances Linéiques du Système Ligne-Câble Avec la Méthode des Éléments Finis. Mémoire du Diplôme de Maitrise ès Sciences Appliquées Soutenu en 2017.
- [9] Gogom, M., Mimiesse, M., Nguimbi, G. and Lilonga-Boyenga, D. (2018) Improving Availability of Transit Capacity by the Hybrid Optimization Method. *Journal of Scientific and Engineering Research*, **5**, 1-13.
- [10] Dan Surianu, F. (2009) Determination of the Induced Voltages bby 220 kV Electric Overhead Power Lines Working in Parallel and Narrow Routes. Measurements on the Ground and Mathematical Model. *WSEAS Transactions on Power Systems*, **4**, 264-274.
- [11] Souad, C. (2013) Réseaux Électriques en ses Divers Régimes Cours. Université Virtuelle de Tunis, Montplaisir, 23, 27.
- [12] Boukhenoufa, F., Boukadoum, A., Leulmi, A., et al. (2012) Régulation Optimale de la Tension & Compensation de la Puissance Réactive avec Contraintes de Sécurité, d'un Réseau Électrique, par la Méthode Hybride MPI & AG, Université du 20 Août 1955 et Université Ferhat A., Skikda-Sétif (Algérie), 1-6.
- [13] Betie, A. (2015) Impacts de la Qualité du Système d'Isolation sur la Condition et l'Efficacité des Transformateurs de Puissance. Thèse de l'Université du Québec, Quebec City.